

**SINGULAR LIMIT APPROACH
TO STABILITY AND BIFURCATION FOR
BISTABLE REACTION DIFFUSION SYSTEMS**

YASUMASA NISHIURA

1. Introduction. Patterns with sharp transition layers appear in various fields such as patchiness and segregation in ecosystems [3,10], traveling waves in excitable media [2,4,5, and 22], striking patterns in morphogenesis models [13], dendric patterns in solidification problem [1], and so on.

The most simple but substantial model system, to which most of the above ones fall, is given by the following reaction-diffusion equations in one-dimensional space:

$$(P) \quad \begin{aligned} u_s &= d_1 u_{xx} + f(u, v) \\ v_s &= d_2 v_{xx} + \delta g(u, v) \end{aligned} \quad \text{on } I,$$

where d_1 and d_2 are the diffusion rates of u and v , and δ is the ratio of the reaction rates. The interval I is either $(-l, l)$ or \mathbf{R} . The Neumann boundary conditions $u_x = 0 = v_x$ is added to (P), when $I = (-l, l)$. It is usually assumed in (P) that one of the following conditions holds:

- (a) There is a significant difference in the diffusion rates of u and v .
- (b) There is a significant difference in the reaction rates of u and v .
- (c) There is a combination of (a) and (b).

Most of the symmetry breaking stationary patterns in the framework of Turing's diffusion driven instability fall into the first category. One of the well-known models is the Gierer and Meinhardt equation describing morphogenetic patterns [13]. Propagator-controller systems including a simple skeleton model for the B-Z reaction lie on the second category [23, 5]. It is essential for such systems that one of the components reacts much faster than the other. Formally speaking, the FitzHugh-Nagumo equations belong to the third category in which the second component v does not diffuse and reacts much slower than the first one [8]. However, the qualitative behavior of solutions of the FHN

Received by the editors on April 4, 1988, and in revised form on August 5, 1989.

Copyright ©1991 Rocky Mountain Mathematics Consortium

equations is almost similar to that of propagator-controller systems. For this reason, the FHN equations fall essentially into the second category. Moreover, for this specific model, there are already several results for the stability of the traveling pulses [12,24].

In this paper we focus on the third category where the first component u reacts much faster than the second one v , although u diffuses slower than v . More specifically, we use the new parameters

$$\varepsilon = \sqrt{d_1}, \quad \tau = \delta/\sqrt{d_1}, \quad D = d_2/\delta$$

and rewrite (P) as

$$((P)_{\varepsilon,\tau}) \quad \begin{cases} \varepsilon\tau u_t = \varepsilon^2 u_{xx} + f(u, v) \\ v_t = Dv_{xx} + g(u, v), \end{cases}$$

where we used the new time variable $t = \delta s$. We assume that $\varepsilon (> 0)$ is sufficiently small. Therefore, we can use the singular perturbation method to obtain, for instance, stationary solutions and traveling waves. Moreover, we assume that the nonlinearities f and g are of *bistable* type as in Figure 1. Note that this assumption is not necessary for the existence of layer oscillations in section 2 [20]. The precise assumptions for f and g will be stated later. The parameters τ and ε are called the *relaxation* and *layer* parameters, respectively, since τ controls the ratio of the reaction rates and ε represents the width of the transition layer. Note that $(P)_{\varepsilon,\tau}$ covers all the above three categories, when τ varies in \mathbf{R}_+ . In fact, when $\tau = O(1/\varepsilon)$ (respectively, $O(\varepsilon)$), it belongs to the class (a) (respectively, (b)), and when $\tau = O(1)$, it falls into the class (c). In this sense, we may say that category (c) is the intermediate one between (a) and (b). It should be noted here that the typical patterns observable in the classes (a) and (b) are different: stationary patterns are stable in category (a), while propagating waves are more common in category (b). Roughly speaking, the fronts always settle down somewhere in space for (a); however, they move in some direction for (b). Therefore, one can imagine that some kind of transition process might happen to the structure of solutions when the system shifts from (a) to (b) (i.e., τ decreases in $(P)_{\varepsilon,\tau}$).

Our aim in this paper consists of the following:

- (1) Find the observable patterns in category (c) and clarify their stability properties.
- (2) Describe the transition process when the system shifts from (a) to (b) and, especially, what kind of bifurcation phenomena occurs when τ decreases.

Before stating the third problem, we make a survey of the results in sections 2 and 3. For an appropriately fixed τ , the stable patterns in category (c) drastically change depending on whether I is finite or not. Namely, we have the layer oscillations (spatially inhomogeneous and time periodic solutions) for the finite interval case, while the travelling front solutions appear for the infinite line case. In other words, there appears a *Hopf* bifurcation for the finite case, but a *static* bifurcation of traveling type for the infinite case. Thus, the last problem is

- (3) How the structure of the bifurcating solutions in category (c) is deformed when the length l of the interval becomes infinite.

The answers for problems (1) and (2) are already obtained except Theorem 3.3 in section 3, at least partially, in [11,20] and are summarized in sections 2 and 3. Theorem 3.3 describes the global bifurcation diagram of traveling front solutions for odd symmetric nonlinearities with τ being a bifurcation parameter, which acts as an *organizing center* for the general case. For the third problem, we shall prove in 4 that the behavior of the critical eigenvalues causing the bifurcation is deformed continuously when the length l tends to infinity (Theorem 4.1).

In order to deal with the above problems rigorously, we always face the difficulties coming from the *largeness* of the amplitude (because of the existence of sharp transition layers) and the *smallness* of ε . Nevertheless, at least for the existence of layered solutions, several methods have been developed systematically. For instance, the singular perturbation method (or matched asymptotic method) is one of the most powerful and constructive methods. However, there have been very few unified approaches to treat stability and bifurcation problems for large amplitude singularly perturbed solutions. There are several reasons for this. First of all, since the singularly perturbed solution has a sharp front at each layer position which becomes a discontinuous point as $\varepsilon \downarrow 0$, the eigenfunctions of the linearized problem at the singularly perturbed solution in general do not remain as usual functions when

$\varepsilon \downarrow 0$. Also, one of the linearized equations becomes an algebraic one since the derivative of the second order vanishes as $\varepsilon \downarrow 0$. Secondly, for the bifurcation problem as in (2), we have to control critical eigenvalues (i.e., Re-parts of them are close to zero) of the linearized problem at a singularly perturbed solution *uniformly* with respect to small ε . Despite these degeneracies, the most desirable thing is to find a nice limiting system from which one can extract necessary information on the behavior of the spectrum for small ε .

For that purpose, some blowing up technique is necessary to take advantage of the smallness ε since just formal limiting arguments (when $\varepsilon = 0$, not $\varepsilon \downarrow 0$) bring us insufficient information on stability properties of singularly perturbed solutions.

The basic tool, which will be employed here, to overcome the above difficulties is the *singular limit eigenvalue problem (SLEP)* method which enables us to study stability and bifurcation problems of singularly perturbed solutions [18, 19, 17, and 20]. The key idea of the SLEP method is to reserve the information coming from layers in the form of the *Dirac's point mass* distribution (in one-dimensional case) of the linearized problem as $\varepsilon \downarrow 0$. The weight of each Dirac's point mass plays an important role to determine the behavior of critical eigenvalues. An appropriate ε -scaling of eigenfunctions of the singular Sturm-Liouville problem is crucial to derive the SLEP system (Lemma 2.3 in section 2).

Now we state the assumptions for f and g (Figure 1).

(A.0) f and g are smooth functions of u and v defined on some open set in \mathbf{R}^2 .

(A.1) The nullcline of f is sigmoidal and consists of three continuous curves $u = h_-(v)$, $h_0(v)$, and $h_+(v)$ defined on the intervals I_- , I_0 , and I_+ , respectively. Let $\min I_- = v_{\min}$ and $\max I_+ = v_{\max}$, then the inequalities $h_-(v) < h_0(v) < h_+(v)$ holds for $v \in I^* \equiv (v_{\min}, v_{\max})$, and $h_+(v)$ (respectively, $h_-(v)$) coincides with $h_0(v)$ at only one point $v = v_{\max}$ (respectively, v_{\min}).

(A.2) $J(v)$ has an isolated zero at $v = v^* \in I^*$ such that $dJ/dv < 0$ at $v = v^*$, where $J(v) = \int_{h_-(v)}^{h_+(v)} f(s, v) ds$.

(A.3) The nullcline of g intersects with that of f at three points

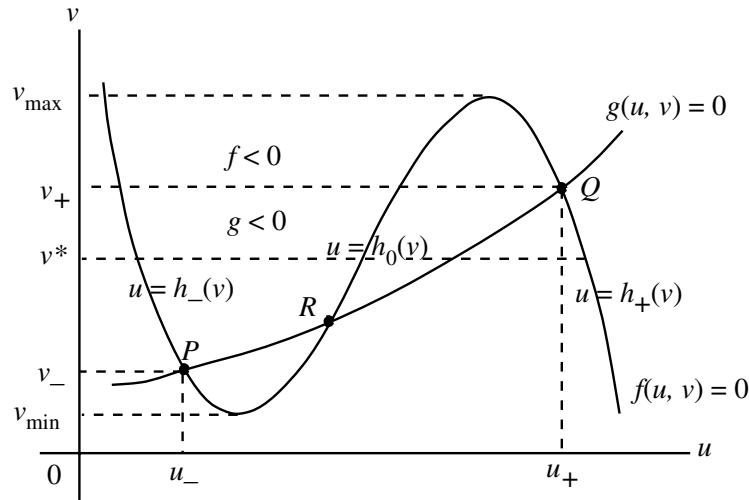


FIGURE 1. Functional forms of f and g .

transversally as in Figure 1. The critical point on $u = h_-(v)$ (respectively, $h_+(v)$ or $h_0(v)$) is denoted by $P = (u_-, v_-) = (h_-(v_-), v_-)$ (respectively, $Q = (u_+, v_+) = (h_+(v_+), v_+)$ or $R = (u_0, v_0) = (h_0(v_0), v_0)$).

(A.4) $f_u < 0$ on $R_+ \cup R_-$, where R_- (respectively, R_+) denotes the part of the curve $u = h_-(v)$ (respectively, $h_+(v)$) defined by

$$R_- \text{ (resp. } R_+) = \{(u, v) \mid u = h_-(v) \text{ (resp. } h_+(v)) \\ \text{for } v_- < v \leq v^* \text{ (resp. } v^* \leq v < v_+)\}$$

(A.5)

(a) $g|_{R_-} < 0 < g|_{R_+}$, (b) $\det \frac{\partial(f, g)}{\partial(u, v)}|_{R_+ \cup R_-} > 0$, (c) $g_v|_{R_+ \cup R_-} \leq 0$.

Remark 1.1. In order to obtain the results in section 2 (layer oscillations), it is not necessary to assume the bistability of f and g . See [20] for the details.

Remark 1.2. The assumption (A.5-b) is equivalent to

$$(1.1) \quad \frac{d}{dv} G_{\pm}(v) < 0,$$

where $G_{\pm}(v)$ is defined by $g(h_{\pm}(v), v)$ since it follows from $f(h_{\pm}(v), v) = 0$ and (A.4) that

$$\frac{d}{dv} G_{\pm}(v) = \frac{f_u g_v - f_v g_u}{f_u} |_{R_{\pm}}.$$

We shall use the following notation throughout the paper. Let I be $(-l, l)$, \mathcal{R}_- , \mathcal{R}_+ , or \mathbf{R} , σ and μ be positive numbers, and let p be a nonnegative integer.

$$C_{\mu} = \{z \in \mathbf{C} \mid \operatorname{Re} z > -\mu\} \text{ for } \mu > 0.$$

$C^p(\bar{I})$ = the space of p -times continuous differentiable functions on \bar{I} with the usual norm.

$C_{\varepsilon}^p(\bar{I})$ = the space of p -times continuous differentiable functions on \bar{I} with the norm

$$\|u\|_{C_{\varepsilon}^p} = \sum_{k=0}^p \max \left| \left(\varepsilon \frac{d}{dk} \right)^k u(x) \right|.$$

$$X_{\mu, \sigma}^p(I) =$$

$$\left\{ u \in C^p(\bar{I}) \mid \|u\|_{X_{\mu, \sigma}^p(I)} = \sum_{i=0}^p \sup_{x \in I} \left| e^{\mu|x|} \left(\sigma \frac{d}{dx} \right)^i u(x) \right| < +\infty \right\}$$

$H^p(I)$ = the usual Sobolev space on I .

$H_N^p(I)$ = the space of closure of $\{\cos(n\pi x)\}_{n=0}^{\infty}$ in $H^p(I)$.

$\langle \cdot, \cdot \rangle$ = the inner product in $L^2(I)$ - space.

2. Layer oscillations, destabilization phenomenon on a finite interval. First we show the existence theorem for the stationary solutions of $(P)_{\varepsilon, \tau}$ on the finite interval $I = (-l, l)$ subject to zero flux boundary conditions and the stability theorem for it when $\tau = 1/\varepsilon$.

Hereafter, we use the abbreviation “SP solution” in place of singularly perturbed solution. Moreover, we assume, for simplicity, that the diffusion coefficient for v is equal to one, i.e., $D = 1$, which does not involve any loss of generality in our setting. The stationary problem for $(P)_{\varepsilon,\tau}$ is given by

$$(SP)_\varepsilon \quad \begin{cases} 0 = \varepsilon^2 u_{xx} + f(u, v) & \text{in } I \\ 0 = v_{xx} + g(u, v) & \\ u_x = 0 = v_x & \text{on } \partial I. \end{cases}$$

Note that $(SP)_\varepsilon$ does not depend on the parameter τ .

Theorem 2.1. (Existence theorem of mono-layered SP solutions, Theorem 1.1 in [18] and references therein.) *There exist $\varepsilon = \varepsilon_0 > 0$ such that $(SP)_\varepsilon$ has an ε -family of mono-layered solutions $\mathcal{U}^\varepsilon = (u(x; \varepsilon), v(x; \varepsilon)) \in C_\varepsilon^2(\bar{I}) \times C^2(\bar{I})$ for $0 < \varepsilon < \varepsilon_0$. They are uniformly bounded in $C_\varepsilon^2(\bar{I}) \times C^2(\bar{I})$ and satisfy*

$$\lim_{\varepsilon \downarrow 0} u(x; \varepsilon) = U_0(x) \quad \text{uniformly on } I \setminus I_\kappa \text{ for any } \kappa > 0,$$

and

$$\lim_{\varepsilon \downarrow 0} v(x; \varepsilon) = V_0(x) \quad \text{uniformly on } I,$$

where $I_\kappa = (x_1^* - \kappa, x_1^* + \kappa)$ and x_1^* denotes the layer position of the reduced solution $\mathcal{U}^* \equiv (U_0, V_0)$ (see Figure 2).

Theorem 2.2 (Stability theorem of mono-layered SP solutions for $\tau = 1/\varepsilon$, Main Theorem in [18]). *SP solutions in Theorem 2.1 are asymptotically stable as stationary solutions of the evolutionary system*

$$(P)_{\varepsilon,1/\varepsilon} \quad \begin{cases} u_t = \varepsilon^2 u_{xx} + f(u, v) & \text{in } I \\ v_t = v_{xx} + g(u, v) & \\ u_x = 0 = v_x & \text{on } \partial I \end{cases}$$

More precisely, there exists a unique critical eigenvalue $\lambda_c(\varepsilon)$ of the linearized eigenvalue problem at $\mathcal{U}^\varepsilon(LP)_{\varepsilon,1/\varepsilon}$ such that

$$(2.1) \quad \lambda_c(\varepsilon) \simeq -\tau_N^* \varepsilon \quad \text{as } \varepsilon \downarrow 0,$$

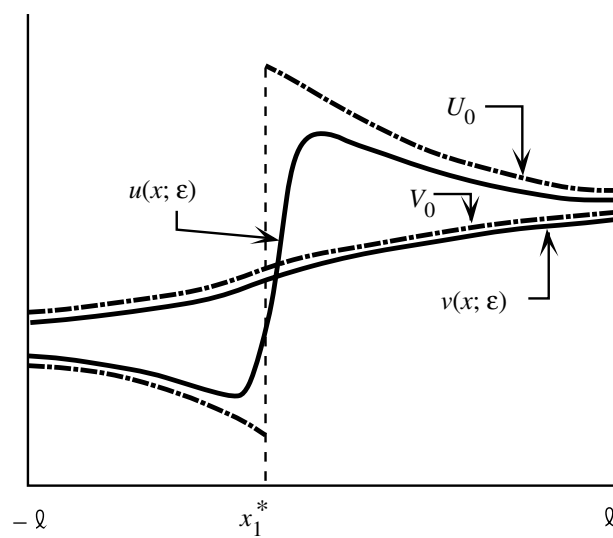


FIGURE 2. Reduced solution and mono-layered SP solution.

where τ_N^* is a positive constant given by

$$(2.2) \quad \tau_N^* = A(0, 0) - \xi_0^* > 0 \quad ((2.6), (2.19)).$$

All the other spectrum have strictly negative Re-parts uniformly for small ε .

Although Theorem 2.2 guarantees the stability of \mathcal{U}^ε when $\tau = 1/\varepsilon$ (Figure 3(a)), the transition layer of \mathcal{U}^ε can be destabilized by speeding up the reaction rate of the u -component in $(P)_{\varepsilon, \tau}$ -system. In fact, when τ becomes small, the stationary front loses its stability and the de-stabilized front oscillates back and forth on a finite interval (Figure 3(b)). We shall study this instability phenomenon by using the SLEP method. The complete proofs for the results in this section are given in [18,20].

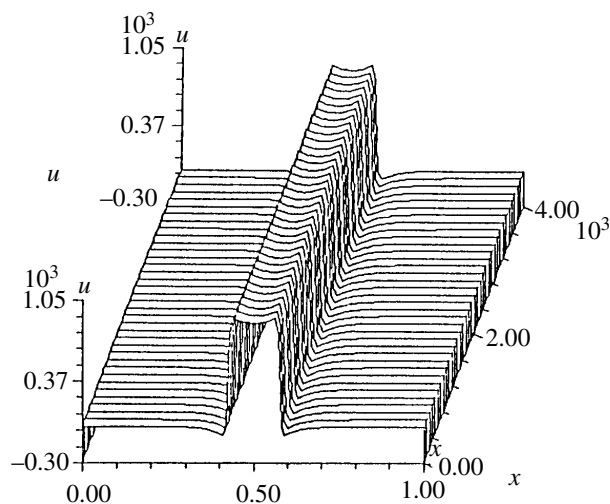


FIGURE 3a. Stable stationary pattern for large τ .

The linearized problem at \mathcal{U}^ε is given by

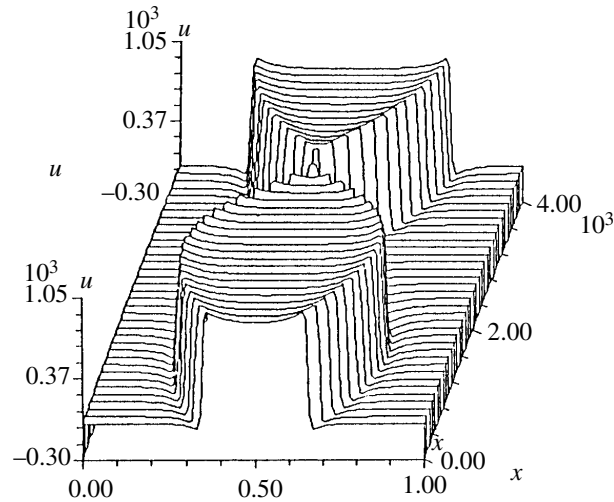
$$(LP)_{\varepsilon,\tau} \begin{cases} \mathcal{L}^{\varepsilon,\tau} \begin{pmatrix} w \\ z \end{pmatrix} = \begin{bmatrix} L^\varepsilon & f_v^\varepsilon \\ g_u^\varepsilon & M^\varepsilon \end{bmatrix} \begin{pmatrix} w \\ z \end{pmatrix} = \lambda \begin{pmatrix} \varepsilon\tau & 0 \\ 0 & 1 \end{pmatrix} \begin{pmatrix} w \\ z \end{pmatrix} & \text{in } I, \\ w_x = 0 = z_x & \text{on } \partial I, \\ \begin{pmatrix} w \\ z \end{pmatrix} \in (H^2(I) \cap H_N^1(I))^2, \end{cases}$$

where

$$L^\varepsilon \equiv \varepsilon^2 \frac{d^2}{dx^2} + f_u^\varepsilon \quad \text{and} \quad M^\varepsilon \equiv \frac{d^2}{dx^2} + g_v^\varepsilon,$$

and partial derivatives $f_u^\varepsilon, g_u^\varepsilon$, etc., are evaluated at the SP solution \mathcal{U}^ε . Since $(P)_{\varepsilon,\tau}$ is a parabolic system for $\varepsilon > 0$, the Re-parts of the spectrum of $(LP)_{\varepsilon,\tau}$ determine the nonlinear stability (or instability) of SP solutions [9]. Therefore, it suffices to consider the spectrum of $(LP)_{\varepsilon,\tau}$ in $C_\mu \equiv \{z \in \mathbf{C} | \text{Re } z > -\mu\}$ with μ being an appropriate positive constant.

Our strategy to solve $(LP)_{\varepsilon,\tau}$ is the following. First we solve the first equation for w and then substitute it into the second equation. We

FIGURE 3b. Layer oscillation for small τ .

divide the resulting equation into the singular part and the nonsingular one and characterize the asymptotic form of each term as $\varepsilon \downarrow 0$. The limiting eigenvalue problem (called the SLEP equation) keeps the essential information by which we can control the behaviors of the critical eigenvalues.

In order to understand the essence of the SLEP method, we first proceed along the above line formally, and, when we encounter the difficulties on the way to the final goal, we present several key lemmas to overcome them. Solving the first equation of $(LP)_{\varepsilon, \tau}$ for w , and substituting it into the second one, we have

$$(2.3) \quad M^\varepsilon z + g_u^\varepsilon (L^\varepsilon - \varepsilon \tau \lambda)^{-1} (-f_v^\varepsilon z) = \lambda z.$$

The first question may be on the existence of the resolvent $(L^\varepsilon - \varepsilon \tau \lambda)^{-1}$. We need the following lemma to answer it.

Lemma 2.1. (See Lemmas 1.4 and 2.1 in [18], and Remark 2.2 in [20]) (a) Let $\{\zeta_n^\varepsilon, \varphi_n^\varepsilon\}_{n \geq 0}$ be the complete orthonormal set of eigenvalues and eigenfunctions (in L^2 -sense) of the following Sturm-Liouville problem

$$(2.4) \quad \begin{aligned} L^\varepsilon \varphi &= \zeta \varphi \quad \text{in } I, \\ \varphi_x &= 0 \quad \text{on } \partial I. \end{aligned}$$

Then it holds that

$$(2.5) \quad \begin{aligned} \zeta_0^\varepsilon &> 0 > \zeta_1^\varepsilon > \dots > \zeta_n^\varepsilon \dots, \\ \zeta_0^\varepsilon &= \hat{\zeta}_0^\varepsilon \varepsilon + \text{Exp}(\varepsilon), \\ \zeta_1^\varepsilon &< -\Delta^* < 0, \quad (\Delta^* > 0 \text{ is independent of } \varepsilon), \end{aligned}$$

where $\hat{\zeta}_0^\varepsilon$ is a positive continuous function up to $\varepsilon = 0$ and

$$(2.6) \quad \begin{aligned} \hat{\zeta}_0^* &\equiv \lim_{\varepsilon \downarrow 0} \hat{\zeta}_0^\varepsilon = (\kappa^*)^2 \frac{dJ}{dv}(v^*) \int_{-l}^{x_1^*} g(U_0, V_0) dx > 0, \\ |\text{Exp}(\varepsilon)| &\leq C \exp(-\gamma/\varepsilon), \quad \gamma > 0, \end{aligned}$$

where $x_1^* \in I$ is the layer position of the reduced solution (U_0, V_0) , and $\kappa^* \equiv \|W_y(y; 0, v^*)\|_{L^2(\mathbf{R})}^{-1} > 0$. Here $W(y; 0, v^*)$ (Lemma 3.2 in 3) is the unique solution (up to translation) of

$$(2.7) \quad W_{yy} + f(W, v^*) = 0 \quad \text{with } W(\pm\infty) = h_\pm(v^*).$$

(b) $\int_I \varphi_0^\varepsilon dx = L(\varepsilon)\sqrt{\varepsilon}$, where $L(\varepsilon)$ is a positive continuous function for $0 \leq \varepsilon < \varepsilon_0$. Moreover,

$$L^* \equiv L(0) = \kappa^*(h_+(v^*) - h_-(v^*)) > 0.$$

(c) $\lambda = \zeta_0^\varepsilon/\varepsilon\tau$ does not belong to the spectrum of $(LP)_{\varepsilon,\tau}$.

Using the eigenfunction expansion of Lemma 2.1, we see that (2.3) becomes

$$(2.8) \quad M^\varepsilon z + g_u^\varepsilon \frac{\langle -f_v^\varepsilon, \varphi_0^\varepsilon \rangle}{\zeta_0^\varepsilon - \varepsilon\tau\lambda} \varphi_0^\varepsilon + g_u^\varepsilon (L^\varepsilon - \varepsilon\tau\lambda)^\dagger (-f_v^\varepsilon z) = \lambda z,$$

where $(L^\varepsilon - \varepsilon\tau\lambda)^\dagger h \equiv \sum_{n \geq 1} (\langle h, \varphi_n^\varepsilon \rangle / \zeta_0^\varepsilon - \varepsilon\tau\lambda) \varphi_n^\varepsilon$. The reason why we pick out the first term of the expansion is that it becomes *singular* in the sense that both the denominator and the numerator of it tend to zero as $\varepsilon \downarrow 0$ (Lemma 2.1). On the other hand, the dagger part of the resolvent does not have such singular terms, and, in fact, it is a uniformly bounded operator from $L^2(I)$ to $L^2(I)$ for small $\varepsilon > 0$. Moreover, it has the following asymptotic characterization.

Lemma 2.2 (Lemma 2.2 in [18]). *Let $F(u, v)$ be a smooth function of u and v . Then*

$$(L^\varepsilon - \varepsilon\tau\lambda)^\dagger (F^\varepsilon h) \xrightarrow{\varepsilon \downarrow 0} F^* h / f_u^* \quad \text{in strong } L^2\text{-sense}$$

for any function $h \in L^2(I) \cap L^\infty(I)$, $\tau \in \mathbf{R}$, and $\lambda \in \mathbf{C}$, where $f_u^* \equiv f_u(U_0, V_0)$, $F^\varepsilon \equiv F(\mathcal{U}^\varepsilon) = F(u(x; \varepsilon), v(x; \varepsilon))$ and $F^* \equiv F(U_0, V_0)$. The convergence is uniform on a bounded set of $\mathbf{C} \times H^1(I)$ with respect to (λ, h) .

Roughly speaking, this lemma says that $(L^\varepsilon - \varepsilon\tau\lambda)^\dagger$ converges to the multiplication operator as $\varepsilon \downarrow 0$. Using this lemma, we have

$$(2.9) \quad \lim_{\varepsilon \downarrow 0} g_u^\varepsilon (L^\varepsilon - \varepsilon\tau\lambda)^\dagger (-f_v^\varepsilon z) = -\frac{g_u^* f_v^*}{f_u^*} z.$$

Thus, the asymptotic characterization of the second term of the left-hand side of (2.8), the *singular part*, is crucial to obtain a nice limiting problem. First we make the following ε -scaling of the singular part.

$$(2.10) \quad [\text{the second term of (2.8)}] = \frac{\langle z, -f_v^\varepsilon \varphi_0^\varepsilon / \sqrt{\varepsilon} \rangle}{\zeta_0^\varepsilon / \varepsilon - \tau\lambda} g_u^\varepsilon \varphi_0^\varepsilon / \sqrt{\varepsilon}.$$

The key idea lies in the next lemma.

Lemma 2.3. (Lemma 2.3 in [18])

$$(a) \quad \lim_{\varepsilon \downarrow 0} \frac{-f_v^\varepsilon}{\sqrt{\varepsilon}} \varphi_0^\varepsilon = c_1^* \delta^*$$

in $H^{-1}(I)$ -sense

$$(b) \quad \lim_{\varepsilon \downarrow 0} \frac{g_u^\varepsilon}{\sqrt{\varepsilon}} \varphi_0^\varepsilon = c_2^* \delta^*$$

where $\delta^* = \delta(x - x_1^*)$ is the Dirac's δ -function at $x = x_1^*$, and

$$\begin{aligned} c_1^* &= -\kappa^* \frac{d}{dv} J(v^*) > 0 \\ c_2^* &= \kappa^* \{g(h_+(v^*), v^*) - g(h_-(v^*), v^*)\} > 0 \end{aligned}$$

with κ^* being the same positive constant as in Lemma 2.1.

Applying this lemma to (2.10), we see that it becomes as $\varepsilon \downarrow 0$

$$(2.11) \quad \hat{c} \frac{\langle z, \delta^* \rangle}{\hat{\zeta}_0^* - \tau \lambda} \delta^*,$$

where $\hat{c} = c_1^* c_2^*$. Combining (2.11) with (2.9) we finally obtain the limiting system of (2.8) as $\varepsilon \downarrow 0$:

$$(2.12) \quad T_\lambda z = \frac{\langle z, \delta^* \rangle \hat{c} \delta^*}{\hat{\zeta}_0^* - \tau \lambda},$$

where

$$T_\lambda \equiv -D \frac{d^2}{dx^2} - \det^* / f_u^* + \lambda, \quad z = z_{\mathbf{R}} + iz_I \quad \text{and} \quad \lambda = \lambda_{\mathbf{R}} + i\lambda_I.$$

Here $\det^* \equiv f_u^* g_v^* - f_v^* g_u^* > 0$ (see (A.5)), $f_u^* \equiv f_u(U_0, V_0)$ and other partial derivatives with $*$ are defined similarly. The equation (2.12) should be written in a weak form since z , in general, belongs to $H_N^1(I)$. However, we write it in a classical form for simplicity. We call (2.12) the *SLEP differential equation* for \mathcal{U}^ε . It may be convenient to convert (2.12) into the transcendental equation with respect to λ and τ . For this purpose, we need the following lemma.

Lemma 2.4 (Lemma 3.1 in [18]). *The operator K_λ (which is, roughly speaking, equal to the inverse of T_λ) is a well-defined uniformly bounded operator from $H^{-1}(I)$ to $H_N^1(I)$ for $\text{Re } \lambda < -\mu_1$. K_λ depends on λ real analytically in operator norm sense where μ_1 is a positive constant satisfying*

$$(2.13) \quad \mu_1 < \inf_{x \in I} \left(-\frac{\det^*}{f_u^*} \right).$$

Applying the inverse operator K_λ of T_λ to (2.12), we have

$$(2.14) \quad z = \frac{\langle z, \delta^* \rangle K_\lambda(\hat{c}\delta^*)}{\hat{\zeta}_0^* - \tau\lambda}$$

which shows that z is a constant multiple of $K_\lambda(\hat{c}\delta^*)$, namely

$$(2.15) \quad z = \alpha K_\lambda(\hat{c}\delta^*)$$

with α being a constant. Substituting (2.15) into (2.14), we see that (2.14) has a nontrivial limiting eigenfunction if and only if τ and λ satisfy the relation

$$(2.16) \quad \hat{\zeta}_0^* - \tau\lambda = \langle K_\lambda(\hat{c}\delta^*), \delta^* \rangle.$$

Let $G(\lambda)$ be defined by the right-hand side of (2.16) and \mathcal{F}^* be defined by

$$(2.17) \quad \mathcal{F}^*(\lambda, \tau) = \hat{\zeta}_0^* - \tau\lambda - G(\lambda).$$

It is obvious that (2.16) is equivalent to look for the solutions of

$$(2.18) \quad \mathcal{F}^*(\lambda, \tau) = 0,$$

which is called the *SLEP equation for \mathcal{U}^ε* . Here \mathcal{F}^* is defined in $\mathbf{C}_{\mu_1} \times \mathbf{R}$. It is clear from the definition that \mathcal{F}^* is analytic with respect to λ and τ .

Remark 2.1. By taking real and imaginary parts of (2.18), we see that it is equivalent to the following:

$$\hat{\zeta}_0^* - \tau\lambda_{\mathbf{R}} - A = 0$$

and

$$\lambda_I(B - \tau) = 0,$$

respectively, where A and B are defined by

$$(2.19)_a \quad A = A(\lambda_{\mathbf{R}}, (\lambda_I)^2) \equiv \langle \hat{I}K_{\lambda_{\mathbf{R}}}(\hat{c}\delta^*), \delta^* \rangle$$

$$(2.19)_b \quad B = B(\lambda_{\mathbf{R}}, (\lambda_I)^2) \equiv \langle \hat{I}K_{\lambda_{\mathbf{R}}}^2(\hat{c}\delta^*), \delta^* \rangle$$

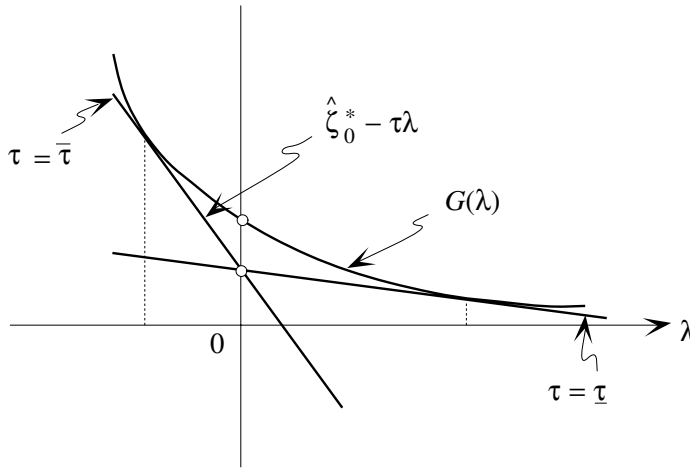


FIGURE 4. Graphs of $\hat{\zeta}_0^* - \tau\lambda$ and $G(\lambda)$.

with $\hat{I} \equiv \{I + (\lambda_I)^2(K_{\lambda_R})^2\}^{-1}$.

Sublemma 2.1. (Lemma 3.2 in [20]). For $\lambda \in \mathbf{C}_{\mu_1}$, both A and B are positive and smooth functions of $\lambda_{\mathbf{R}}$ and $(\lambda_I)^2$ satisfying

- (a) $\frac{\partial A}{\partial (\lambda_I)^2} < 0$ and $\frac{\partial B}{\partial (\lambda_I)^2} < 0$,
- (b) $\lim_{|\lambda_I| \uparrow \infty} A = 0$ and $\lim_{|\lambda_I| \uparrow \infty} B = 0$.

Moreover, B satisfies

- (c) $\frac{\partial B}{\partial \lambda_{\mathbf{R}}} < 0$ in \mathbf{C}_{μ_1} .

Although we delegate the detailed analysis of (2.18) to [20], it is instructive to consider it on a real line. $G(\lambda)$ satisfies the following properties as a function of $\lambda \in \mathbf{R}$.

Lemma 2.5. (Lemma 3.3 in [20]). $G(\lambda)$ is a positive, strictly decreasing and convex function for $\lambda(\geq -\mu_1) \in \mathbf{R}$ with $\lim_{\lambda \uparrow \infty} G(\lambda) = 0$ (see Figure 4).

As far as the real solutions of (2.18) are concerned, we see from (2.16) that they are given by the intersecting points between the straight line $\hat{\zeta}_0^* - \tau\lambda$ and the convex curve $G(\lambda)$. Note that $G(0) > \hat{\zeta}_0^*$ from (2.2). When τ varies, we easily see by simple geometrical consideration that there exist two values $\underline{\tau}$ and $\bar{\tau}$ such that there are no real intersections for $\underline{\tau} < \tau < \bar{\tau}$. When $\tau > \bar{\tau}$, there are two negative intersections $\lambda_c^0(\tau)$ and $\lambda_c^1(\tau)$ with $0 > \lambda_c^0(\tau) > \lambda_c^1(\tau)$. On the other hand, when $\tau < \underline{\tau}$, there are two positive one $\lambda_c^0(\tau)$ and $\lambda_c^1(\tau)$ with $0 < \lambda_c^0(\tau) < \lambda_c^1(\tau)$. Here we always denote by $\lambda_c^0(\tau)$ the real solution closer to zero (see also Figure 12 in §4). Moreover, these two curves are tangent with each other at positive (respectively, negative) real value when $\tau = \underline{\tau}$ (respectively, $\bar{\tau}$). See Figure 4. One can imagine that, when τ decreases from $\bar{\tau}$, the real solutions split into a pair of complex conjugate eigenvalues, cross the imaginary axis, and fall again to the real axis at $\tau = \underline{\tau}$. Namely, both real eigenvalues $\lambda_c^0(\tau)$ and $\lambda_c^1(\tau)$ are extended to be complex ones as a function of τ like Figure 5. This is true as in the following main theorem in this section.

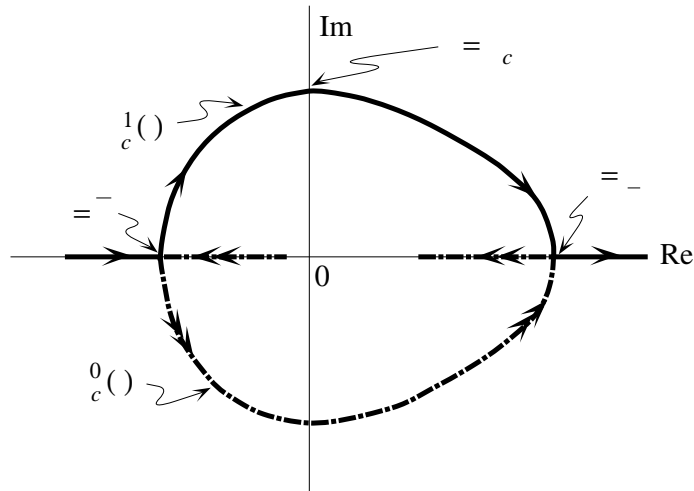
Theorem 2.3. (Theorem 3.1 in [20]). (a) *There exists a unique τ_c such that a unique isolated pair of complex eigenvalues $\lambda_c^0(\tau)$ and $\lambda_c^1(\tau)$ ($= \overline{\lambda_c^0(\tau)}$) with $\text{Im } \lambda_c^0(\tau) < 0$ of (2.18) cross the imaginary axis transversally from left to right at $\tau = \tau_c$, when τ decreases.*

(b) *At $\tau = \tau_c$, all the remaining spectrum of (2.18) lies strictly in the left-half plane in \mathbf{C} , namely, the Hopf-instability occurs primarily.*

(c) *After the Hopf bifurcation, the pure imaginary eigenvalues behave as in Figure 5. Namely, $\lambda_c^0(\tau)$ and its complex conjugate fall into the real positive eigenvalue of double multiplicity at $\tau = \underline{\tau}$ ($< \tau_c$), and then split into the two real eigenvalues $\lambda_c^0(\tau)$ and $\lambda_c^1(\tau)$ with $\lambda_c^0(\tau) < \lambda_c^1(\tau)$ for $\tau < \underline{\tau}$.*

Moreover, for $\tau \leq \tau_c$, there are no points of the spectrum in $\text{Re } \lambda \geq -\hat{\mu}$ except for those constructed above with some positive constant $\hat{\mu}$.

Using this theorem, we can prove by *regular perturbation* that the Hopf bifurcation also occurs for positive ε (Theorem 4.1 in [20]). Namely, qualitatively speaking, Theorem 2.3 is valid for $\varepsilon > 0$. Numerical pictures of layer oscillations are depicted in Figure 3 and Figure 11. Figure 3 shows the oscillation for the double layer case; however,

FIGURE 5. Behaviors of critical eigenvalues with respect to τ .

it can be regarded as a mono-layer oscillation since the pictures are symmetric at $x = 0$.

Remark 2.2. In section 4, we denote the two critical eigenvalues of Theorem 2.3 by $\lambda_c^{0,\hat{l}}(\tau)$ and $\lambda_c^{1,\hat{l}}(\tau)$ to indicate the $\hat{l}(\equiv l^{-1})$ -dependency, where l is the length of the interval I .

3. Bifurcation of traveling waves. Destabilization phenomenon on the infinite line. When the spatial domain becomes infinite and the kinetics of the nonlinearities is of bistable type like Figure 1, the natural class of solutions which corresponds to the mono-layered static solutions in section 2 is given by that of the traveling front solutions connecting two stable constant states P and Q . The stationary solutions are contained as a special case with zero velocity. Roughly speaking, the *translation invariance* forces us to enlarge the solution space. For the scalar reaction-diffusion equation of bistable type (see, e.g., [6]), it is well established that the traveling front exists uniquely (up to translation) and globally stable for an appropriate class of initial functions. However, for the system of equations like $(P)_{\varepsilon,\tau}$,

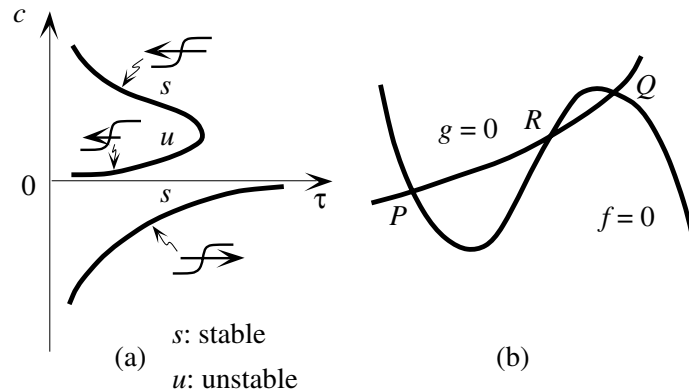


FIGURE 6. Global bifurcation diagram of traveling front solutions for the general case.

these are, in general, *not* true. In fact, there occurs *multiple existence of traveling fronts* for some parameter region of τ , and, therefore, *both stable and unstable traveling fronts coexist simultaneously*. A global bifurcation diagram of traveling fronts for such systems is presented in [11], and stability properties of them are clarified in [21] by using the SLEP method. A typical situation is depicted in Figure 6. It should be noted here that all solutions represented in Figure 6 are traveling front solutions and there are *no* Hopf bifurcations in it (see also Remark 3.4). It is also discussed in [21] how the *stability* properties are related to the *sign of the Jacobian of matching conditions* (3.23), by which we can judge the stability of the traveling front from the construction itself. Practically, this seems to be quite useful. However, we do not yet answer the following basic questions: “What is the origin of the global bifurcation diagram like Figure 6,” and “Why are the bifurcation diagrams so different between the finite interval case and the infinite one”? A key ingredient to answer these questions is to consider the most degenerate case, namely the *odd symmetric case*. More precisely, we say that $(P)_{\varepsilon, \tau}$ has odd symmetry, when the following holds

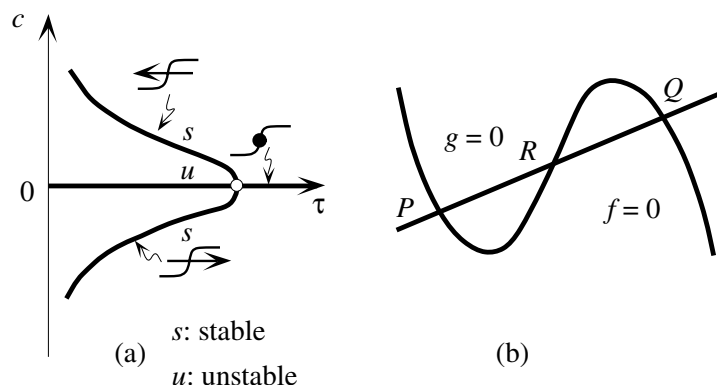


FIGURE 7. Global bifurcation diagram of traveling front solutions for the odd symmetric case.

$$(3.1) \quad \begin{aligned} f(u - u_0, v - v_0) &= -f(-(u - u_0), -(v - v_0)), \\ g(u - u_0, v - v_0) &= -g(-(u - u_0), -(v - v_0)), \end{aligned}$$

where $R = (u_0, v_0)$ is the middle equilibrium point of $f = 0 = g$ (see Figure 7). When $(P)_{\varepsilon, \tau}$ has odd symmetry, the bifurcation diagram changes from Figure 6(a) to Figure 7(a), the *pitchfork bifurcation* (see Proposition 3.1). Apparently, the symmetry of the nonlinearities is inherited to the structure of the bifurcation diagram. Moreover, the general case as in Figure 6(a) can be regarded as an imperfection of Figure 7(a). In this sense, the odd symmetric case may be called the *organizing center*.

In this section, after summarizing the main results of [11] and [21], we shall prove that the diagram Figure 7(a) is true (see Theorem 3.3), i.e., a unique pitchfork bifurcation occurs at $\tau = \tau_c$, and the diagram is invariant under the reverse of the velocity ($c \rightarrow -c$). The metamorphosis from the Hopf bifurcation to the pitchfork one when the length of the interval tends to infinity will be discussed in section 4 (problem (3) in section 1). Combining the results in this section with those in section 4, we can give at least partial answers to the questions stated above.

3.1. *Construction of traveling fronts.* Introducing the traveling coordinate $x = z + ct$ to $(P)_{\varepsilon, \tau}$ in 1, traveling wave solutions with velocity c satisfy

$$(3.2) \quad \begin{cases} \varepsilon^2 u_{xx} - \varepsilon c \tau u_x + f(u, v) = 0 \\ v_{xx} - c v_x + g(u, v) = 0 \end{cases}$$

with boundary conditions

$$(3.3) \quad \begin{cases} u(\pm\infty) = u_{\pm} \\ v(\pm\infty) = v_{\pm}. \end{cases}$$

In order to avoid the phase ambiguity, we impose the following condition on $u(x)$

$$(3.4) \quad u(0) = \alpha,$$

where α is an arbitrarily fixed value in some interval (see (3.11)). Moreover, we put

$$(3.5) \quad v(0) = \beta$$

for $\beta \in (v_-, v_+)$ which will be determined later.

We divide the whole interval \mathbf{R} into two subintervals \mathbf{R}_- and \mathbf{R}_+ and consider the following boundary value problem on each subinterval:

$$(3.6)_{\pm} \quad \begin{cases} \varepsilon^2 (u_{\pm})_{xx} - \varepsilon c \tau (u_{\pm})_x + f(u_{\pm}, v_{\pm}) = 0 \\ (v_{\pm})_{xx} - c (v_{\pm})_x + g(u_{\pm}, v_{\pm}) = 0 \\ u_{\pm}(\pm\infty) = u_{\pm}, \quad u_{\pm}(0) = \alpha \\ v_{\pm}(\pm\infty) = v_{\pm}, \quad v_{\pm}(0) = \beta. \end{cases} \quad x \in \mathbf{R}_{\pm}.$$

Note that c and β are unknown parameters.

The basic idea of the matched asymptotic expansion method is to construct solutions on R_{\pm} separately and then match them smoothly at $x = 0$. We shall do this procedure to the lowest order, i.e. C^1 -matching procedure for outer and inner solutions. The resulting approximate solutions are called the *singular limit traveling front solutions* by which

we are able to construct true solutions for positive ε with the aid of the generalized implicit function theorem ([11] and references therein). As we shall see later, all the essential information necessary for our purpose is contained in the singular limit solutions.

Outer solutions. In the region away from a layered position, the derivatives of u_{\pm} are moderate; therefore, the solutions of the following limiting equations of (3.6) $_{\pm}$ as $\varepsilon \downarrow 0$ become good approximations there.

$$(3.7)_{\pm} \quad \begin{cases} f(u_{\pm}, v_{\pm}) = 0, \\ (v_{\pm})_{xx} - c(v_{\pm})_x + g(u_{\pm}, v_{\pm}) = 0, \\ v_{\pm}(\pm\infty) = v_{\pm}, \quad v_{\pm}(0) = \beta. \end{cases} \quad x \in \mathbf{R}_{\pm}.$$

As particular solutions of the first equation, we can take $u_{\pm} = h_{\pm}(v_{\pm})$ (see (A.1)). Substituting this into the second equation, we see that (3.7) $_{\pm}$ is reduced to

$$(3.8)_{\pm} \quad \begin{cases} (V_{\pm})_{xx} - c(V_{\pm})_x + g(h_{\pm}(V_{\pm}), V_{\pm}) = 0, \\ V_{\pm}(\pm\infty) = v_{\pm}, \quad V_{\pm}(0) = \beta. \end{cases} \quad x \in \mathbf{R}_{\pm},$$

In view of Lemma 2.1 of [11] we see that, for any fixed $c \in \mathbf{R}$ and $\beta \in (v_-, v_+)$, there exists a unique monotone increasing solution of (3.8) $_{\pm}$ denoted by $V_0^{\pm}(x; c, \beta)$ ($x \in \mathbf{R}$), respectively.

In order to match V_0^+ and V_0^- in C^1 -sense at $x = 0$, we have to find $(c, \beta) \in \mathbf{R} \times (v_-, v_+)$ which satisfy

$$(3.9) \quad \psi_0(c, \beta) \equiv \frac{d}{dx} V_0^-(0; c, \beta) - \frac{d}{dx} V_0^+(0; c, \beta) = 0.$$

Lemma 3.1. (The outer relation, see Lemma 2.2 in [11]). *For any fixed $c \in \mathbf{R}$, there uniquely exists $\beta = \beta_0(c)$ satisfying (3.9), which is a smooth strictly monotone decreasing function of $c \in \mathbf{R}$ and converges to v_{\pm} as $c \rightarrow \mp\infty$, respectively. See Figure 8.*

We define $U_0^{\pm}(x; c, \beta)$ by $U_0^{\pm}(x; c, \beta) = h_{\pm}(V_0^{\pm}(x; c, \beta))$, $x \in \mathbf{R}_{\pm}$. Moreover, we denote the C^1 -matching outer solution on the whole line

by $(U_0(x; c), V_0(x; c))$, namely

(3.10)_a

$$V_0(x; c) \equiv \begin{cases} V_0^-(x; c, \beta_0(c)) & x \in \mathbf{R}_- \\ V_0^+(x; c, \beta_0(c)) & x \in \mathbf{R}_+ \end{cases}$$

and

(3.10)_b

$$U_0(x; c) \equiv \begin{cases} h_-(V_0^-(x; c, \beta_0(c))) & x \in \mathbf{R}_- \\ h_+(V_0^+(x; c, \beta_0(c))) & x \in \mathbf{R}_+. \end{cases}$$

Inner solutions. Since the outer solutions $U_0^\pm(x; c, \beta)$ do not satisfy the boundary condition at $x = 0$, we add the inner solutions W_0^\pm to U_0^\pm in a neighborhood of $x = 0$. For this purpose, it is convenient to introduce the stretched variable $y = x/\varepsilon$. Substituting $(U_0^\pm + W_0^\pm, V_0^\pm)$ into (2.5)_± and putting $\varepsilon = 0$, we obtain the following:

$$(3.11)_\pm \quad \begin{cases} (W_0^\pm)_{yy} - c\tau(W_0^\pm)_y + f(h_\pm(\beta) + W_0^\pm, \beta) = 0, & y \in \mathbf{R}_\pm, \\ W_0^\pm(0) = \alpha - h_\pm(\beta), \\ W_0^\pm(\pm\infty) = 0, \end{cases}$$

where β and α are fixed constants satisfying $\beta \in (v_-, v_+)$ and $\alpha \in (h_-(\beta), h_+(\beta))$. By virtue of Lemma 2.4 in [11], we see that (3.11)_± have unique strictly monotone increasing solutions $W_0^\pm(y; c\tau, \beta)$. The inner transition layer on the whole line connecting $h_-(\beta)$ to $h_+(\beta)$ is essentially obtained by the following:

Lemma 3.2. (See [6]). *For any $\beta \in [v_-, v_+]$, consider the following problem:*

$$(3.12) \quad \begin{cases} W_{yy} - cW_y + f(W, \beta) = 0, & y \in \mathbf{R} \\ W(\pm\infty) = h_\pm(\beta), & W(0) = \alpha. \end{cases}$$

Then there exists $c = c_0(\beta)$ such that (3.12) has a unique strictly monotone increasing solution $W(y; c_0(\beta), \beta)$ satisfying

$$|W(y; c_0(\beta), \beta) - h_\pm(\beta)| \in X_{\sigma_\pm(\beta), 1}^2(\mathbf{R}_\pm),$$

where

$$\sigma_{\pm}(\beta) = [\mp c_0(\beta) + \sqrt{(c_0(\beta))^2 - 4f_u(h_{\pm}(\beta), \beta)}] / 2$$

and

$$c_0(\beta) \leq 0 \text{ if and only if } J(\beta) \leq 0 \quad (\text{see (A.2)}).$$

In order to match W_0^+ and W_0^- in C^1 -sense at $x = 0$, we have to find $(c, \beta) \in \mathbf{R} \times (v_{\min}, v_{\max})$ which satisfy

$$(3.13) \quad \phi_0(c, \beta) = \frac{d}{dy} W_0^-(0; c\tau, \beta) - \frac{d}{dy} W_0^+(0; c\tau, \beta).$$

It is almost clear from Lemma 3.2 that the derivatives of W_0^+ and W_0^- are matched at $x = 0$ if and only if c is equal to $c_0(\beta)/\tau$, which gives rise to the second relation between c and β .

Here we assume, for simplicity, the following

$$(A.6) \quad f_v(u, v) < 0 \quad \text{for } (u, v) \in \{(u, v) \mid h_-(v) \leq u \leq h_+(v), v_- \leq v \leq v_+\}.$$

This guarantees the monotonicity of the next inner matching relation.

Lemma 3.3. (The inner relation, see Lemma 2.4 in [11]). *For any fixed $\beta \in [v_-, v_+]$, there exists a unique $c = c_I(\beta; \tau)$ defined by*

$$(3.14) \quad c_I(\beta; \tau) \equiv c_0(\beta)/\tau,$$

which satisfies (3.13). Moreover, under (A.6), it is a strictly monotone decreasing function of β for any τ . See Figure 8.

Remark 3.1. It follows from Lemma 3.3 that $dc_I(\beta, \tau)/d\beta$

($= 1/\tau dc_0(\beta)/d\beta$) is strictly negative for $\beta \in [v_-, v_+]$. Therefore, there exists an inverse function of (3.14):

$$(3.15) \quad \beta = \beta_I(c; \tau) (\equiv c_0^{-1}(c\tau)),$$

which is strictly decreasing for $c \in (c_I(v_+; \tau), c_I(v_-; \tau))$.

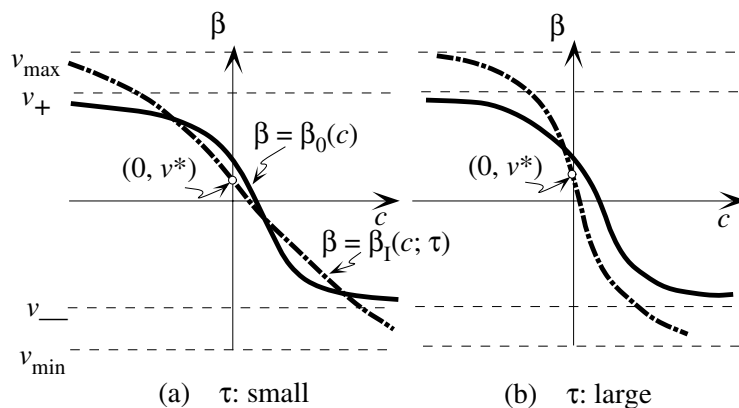


FIGURE 8. Intersections of the outer and inner relations.

Remark 3.2. The definition domain for β can be extended to (v_{\min}, v_{\max}) in Lemma 3.3, since Lemma 3.2 holds for $\beta \in (v_{\min}, v_{\max})$.

The singular limit traveling waves are obtained by taking the common zeros of outer and inner matching conditions:

$$(3.16) \quad \phi_0(c, \beta) = 0 = \psi_0(c, \beta).$$

In view of Lemmas 3.1 and 3.3, this is equivalent to finding the intersection of two graphs:

$$(3.17) \quad \beta = \beta_0(c) \quad \text{and} \quad \beta = \beta_I(c; \tau) \quad (\equiv c_0^{-1}(c\tau)).$$

For any given $\tau > 0$, let (c^*, β^*) be an arbitrary intersection point of (3.17). Define $(u_0(x; \varepsilon, \tau), v_0(x; \varepsilon, \tau))$ by

$$(3.18)_a \quad u_0(x; \varepsilon, \tau) = \begin{cases} U_0^-(x; c^*, \beta^*) + W_0^-(\frac{x}{\varepsilon}; \tau, c^*, \beta^*), & x \in \mathbf{R}_- \\ U_0^+(x; c^*, \beta^*) + W_0^+(\frac{x}{\varepsilon}; \tau, c^*, \beta^*), & x \in \mathbf{R}_+ \end{cases}$$

and

$$(3.18)_b \quad v_0(x; \varepsilon, \tau) = \begin{cases} V_0^-(x; c^*, \beta^*), & x \in \mathbf{R}_- \\ V_0^+(x; c^*, \beta^*), & x \in \mathbf{R}_+. \end{cases}$$

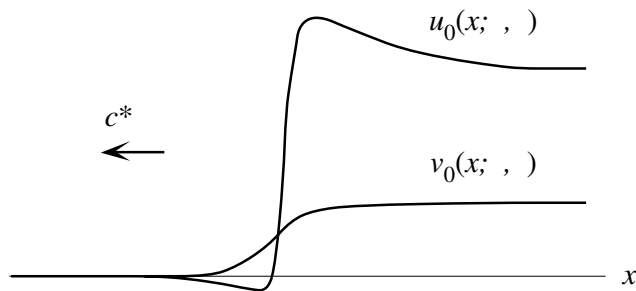


FIGURE 9. Singular limit traveling front solution.

We call $(u_0(x; \varepsilon, \tau), v_0(x; \varepsilon, \tau))$ a *singular limit traveling front solution* of (3.2), (3.3) and (3.4). See Figure 9. The traveling speed c^* is called the *singular limit velocity*.

Depending on τ and the location of v^* (see (A.2)), the number of the singular limit traveling wave solutions vary in the following way.

Theorem 3.1. *Suppose that (A.0)–(A.6) hold. When $v^* \in (v_-, v_+)$, (3.2), (3.3) and (3.4) have three singular limit traveling wave solutions for small τ and have only one for large τ (Figure 8). On the other hand, when $v^* \in (v_{\min}, v_{\max}) \setminus (v_-, v_+)$, it has only one for both small and large τ .*

When the following nondegenerate condition

$$(3.19) \quad \frac{\partial(\phi_0, \psi_0)}{\partial(c, \beta)} \Big|_{(c, \beta) = (c^*, \beta^*)} \neq 0$$

is satisfied, the exact solutions for positive ε can be constructed from the singular limit traveling front solutions. Note that (3.19) is equivalent to

$$(3.20) \quad \text{The two curves } \beta = \beta_0(c) \text{ and } \beta = \beta_I(c; \tau) \text{ intersect transversally at } (c, \beta) = (c^*, \beta^*).$$

Theorem 3.2. (Theorem 3.1 in [11]). *Suppose that (A.0)–(A.6) hold and that (3.19) (or (3.20)) holds at (c^*, β^*) for a given τ . Then, for any $\varepsilon \in (0, \varepsilon_0)$, there exists a traveling wave solution $\mathcal{U}^\varepsilon = (u^\varepsilon, v^\varepsilon) = (u(x; \varepsilon, \tau), v(x; \varepsilon, \tau))$ of the problem (3.2), (3.3) and (3.4) which satisfies*

$$\|u(\cdot; \varepsilon; \tau) - u_0(\cdot; \varepsilon; \tau)\|_{X_{\rho, \varepsilon}^1(\mathbf{R})} + \|v(\cdot; \varepsilon; \tau) - v_0(\cdot; \varepsilon; \tau)\|_{X_{\rho, 1}^1(\mathbf{R})} \rightarrow 0$$

as $\varepsilon \downarrow 0$. Furthermore, the velocity $c(\varepsilon; \tau)$ converges to the singular velocity c^* as $\varepsilon \downarrow 0$.

3.2. *Global bifurcation diagram for singular limit traveling fronts.* Since both relations of (3.17) are strictly monotone decreasing with respect to c we can label each singular limit solution by its velocity c^* in one-to-one fashion. Therefore, we can draw a bifurcation diagram in (c, τ) -plane with τ being a bifurcation parameter. In view of Lemma 3.3, we see that the parameter τ controls the scaling of the c -axis. For example, when τ is small, the graph of β_I is stretched along the c -axis (Figure 8). Therefore, the typical global bifurcation diagram is given by Figure 6(a) ([11] for the details). On the other hand, we have the following for the odd symmetric case.

Theorem 3.3. (Global bifurcation diagram for the odd symmetric case). *Suppose that f and g satisfy (3.1). Then the global bifurcation diagram for singular limit traveling front solutions in (c, τ) -plane satisfies the following properties besides those mentioned in Theorem 3.1 (Figure 7(a)):*

- (a) *There is a trivial branch $c = 0$ independent of τ which corresponds to the standing front solution.*
- (b) *The diagram is invariant under the reverse of the sign of the velocity ($c \rightarrow -c$).*
- (c) *There exists a unique τ_c such that a pitchfork bifurcation (from $c \equiv 0$) occurs at $(c, \tau) = (0, \tau_c)$.*

Proof. Using the odd symmetry of the nonlinearities, it is not difficult to show that both $\beta = \beta_0(c)$ and $\beta = \beta_I(c; \tau)$ are also odd symmetric at $(c, \beta) = (0, v^*)$. Note that both graphs go through the point $(0, v^*)$ under (3.1). Therefore, (a) and (b) follow directly from this observation.

As for (c), we first expand $\beta_0(c)$ and $\beta_1(c; \tau) (\equiv c_0^{-1}(c\tau))$ into Taylor series at $c = 0$:

$$(3.21) \quad \begin{aligned} \beta_0(c) &= v^* + a_1c + \frac{a_3}{3!}c^3 + \cdots + \frac{a_{2k+1}}{(2k+1)!}c^{2k+1} + \cdots, \\ \beta_1(c; \tau) &= v^* + b_1(c\tau) + \frac{b_3}{3!}(c\tau)^3 + \cdots + \frac{b_{2k+1}}{(2k+1)!}(c\tau)^{2k+1} + \cdots, \end{aligned}$$

where $a_{2k+1} = \frac{d^{2k+1}}{dc^{2k+1}}\beta_0(0)$ and $b_{2k+1} = (d^{2k+1}/d(c\tau)^{2k+1})c_0^{-1}(0)$. Note that even powers do not appear because of odd symmetry. The intersection points of $\beta_0(c)$ and $\beta_1(c; \tau)$ are given by the zeros of

$$(3.22) \quad (a_1 - b_1\tau)c + \frac{1}{3!}(a_3 - b_3\tau^3)c^3 + \cdots = 0.$$

In view of Lemmas 3.1 and 3.3, we see that both a_1 and b_1 are strictly negative. We define τ_c by $\tau_c \equiv a_1/b_1 > 0$. Then it follows from (3.22) that $(c, \tau) = (0, \tau_c)$ becomes a pitchfork bifurcation point with the branch $\hat{\tau} (\equiv \tau - \tau_c) \simeq \frac{1}{3!b_1}(a_3 - b_3\tau_c^3)c^2$ as well as the trivial branch $c = 0$. Apparently, the direction of the bifurcation is determined by the sign of $a_3 - b_3\tau_c^3$. It may happen that $a_3 - b_3\tau_c^3 = 0$. In this case we have to take into account the higher order terms (i.e., the first nonzero term at $\tau = \tau_c$). However, we do not go into this further since such a case is not generic. \square

Remark 3.3. Theorem 3.3 can be obtained also through the bifurcation analysis of (3.2) at the standing front with $c = 0$. As we shall see in the next subsection, the standing front loses its stability at $\tau = \tau_c$. In fact, a simple real eigenvalue crosses the origin transversally beside the zero translation free eigenvalue. More precise analysis is done in the paper ‘‘Heteroclinic and homoclinic bifurcations in bistable reaction diffusion systems’’ by H. Kokubu, Y. Nishiura, and H. Oka (J. Differential Equations **86** (2) (1990), 260–341) which puts emphasis on the geometric aspects of bifurcation and stability.

3.3 Stability and matching conditions. Stability of each traveling wave in the previous subsection can be determined by using the SLEP method as in section 2. The associated linearized eigenvalue problem has always the *zero* eigenvalue coming from the translation invariance,

which is one of the major difference from the case in section 2, and its eigenfunction is given by the spatial derivative of the traveling front solution. It turns out that the number of the eigenvalues crucial to the stability is equal to two, but both are *real* ones. There do not appear complex eigenvalues as far as *mono*-front solutions are concerned (see also Remark 3.5). Since one of them is always a zero eigenvalue mentioned above, the other one essentially determines the stability. The location of this real critical eigenvalue varies when the solution varies, say, according to τ . However, it can be proved as in the next theorem that the sign of the Jacobian of matching conditions is closely related to that of the critical eigenvalue.

Theorem 3.4. (Stability of the Traveling Front Solutions [21]). *Let \mathcal{U}^ε be an arbitrary traveling front solution of (3.2)–(3.4), and its singular limit solution corresponds to the intersection point (c^*, β^*) of the outer and the inner matching conditions (3.17). Assume that (c^*, β^*) is a transversal intersection point, namely, $\beta = \beta_0(c)$ and $\beta = \beta_I(c; \tau)$ intersect transversally there (or equivalently (3.19)). Then, the linearized eigenvalue problem of $(P)_{\varepsilon, \tau}$ at \mathcal{U}^ε (for instance, in $C_{\text{unif}}(\mathbf{R})$ (= the set of uniform continuous functions on \mathbf{R})) has only one real critical eigenvalue $\lambda_c^{1, \varepsilon}(\tau)$ for small ε besides the simple zero translation free eigenvalue and all the remaining spectrum have strictly negative real parts. The sign of $\lambda_c^{1, \varepsilon}(\tau)$, which determines the stability of \mathcal{U}^ε , can be judged through the following equivalence of relations:*

$$(3.23) \quad \lambda_c^{1, \varepsilon} \leq 0 \leftrightarrow \frac{d\beta_I}{dc}(c^*; \tau) \geq \frac{d\beta_0}{dc}(c^*) \leftrightarrow \frac{\partial(\phi_0, \psi_0)}{\partial(c, \beta)} \geq 0 \quad \text{at } (c^*, \beta^*).$$

Remark 3.4. Using the equivalence relation (3.23), we can conclude from Figure 8 that the stability property of each solution in Figures 6 and 7 is true.

In the following, we present the final form of the SLEP equation for \mathcal{U}^ε , although we delegate its derivation to [21]. Applying a similar procedure as in section 2 to the linearized problem at \mathcal{U}^ε , the transcendental equation with respect to the critical eigenvalue λ and τ , i.e., the SLEP equation, is given by

$$(3.24) \quad \hat{\zeta}_0^* - \tau\lambda = G(\lambda; c^*, \tau),$$

where

$$(3.25) \quad \hat{\zeta}_0^* = -\frac{dc_0(\beta)}{d\beta} \left\{ c^*(\beta^* - v_-) - \int_{-\infty}^0 g(U_0, V_0) dx \right\},$$

$$(3.26) \quad G(\lambda; c^*, \tau) \equiv k_1^* k_2^* \langle K_\lambda^{*,\tau,c^*} \delta^*, \delta^* \rangle,$$

δ^* is the Dirac's point mass at $x = 0$, k_1^* and k_2^* are defined by

(3.27)

$$k_1^* = -\|W_y^*(y; c_0(\beta^*), \beta^*)\|_{L^2}^{-1} \langle W_y, W_y^* \rangle \frac{d}{d\beta} c_0(\beta^*) > 0,$$

$$k_2^* = \|W_y(y; c_0(\beta^*), \beta^*)\|_{L^2}^{-1} \{g(h_+(\beta^*), \beta^*) - g(h_-(\beta^*), \beta^*)\} > 0,$$

where W_y^* is defined by $\{\exp(-c_0(\beta^*))y\}W_y$, and finally, K_λ^{*,τ,c^*} denotes the inverse of the differential operator

$$-\left\{ \frac{d^2}{dx^2} - c^* \frac{d}{dx} + \frac{\det^*}{f_u^*} - \lambda \right\}$$

where $\det^* \equiv f_u^* g_v^* - f_v^* g_u^*$, $f_u^* \equiv f_u(U_0, V_0)$, and (U_0, V_0) is the outer solution for $\mathcal{U}^{\varepsilon,\tau}$ (see (3.10)). G , as a function of λ , satisfies the following.

Lemma 3.4. (Functional form of $G(\lambda; c^*, \tau)$, [21]). *$G(\lambda; c^*, \tau)$ is a positive, strictly decreasing, and convex function of $\lambda(\geq -\mu_1) \in \mathbf{R}$ with $\lim_{\lambda \uparrow \infty} G(\lambda; c^*, \tau) = 0$, where μ_1 is defined similarly as in (2.11). Moreover, it holds that $G(0; c^*, \tau) = \hat{\zeta}_0^*$. See Figure 10.*

Recalling Lemma 2.5 and Figure 4, we see from Lemma 3.4 that a remarkable difference between (2.16) and (3.24) is that $\lambda = 0$ is always an intersection point of $\hat{\zeta}_0^* - \tau\lambda$ and $G(\lambda; c^*, \tau)$ of (3.24). Therefore, one can expect that another intersection point denoted by $\lambda_c^1(\tau)$ essentially determines the stability. Moreover, we see from Figure 10 that the inequality $-\tau \geq \frac{d}{d\lambda} G(0; c^*, \tau)$ related to the slopes at $\lambda = 0$ is equivalent to $\lambda_c^1(\tau) \geq 0$. The core part of the proof of Theorem 3.3 is to show that this is also equivalent to (3.23). Once the location of $\lambda_c^1(\tau)$ is determined, it can be extended, by regular perturbation, to the

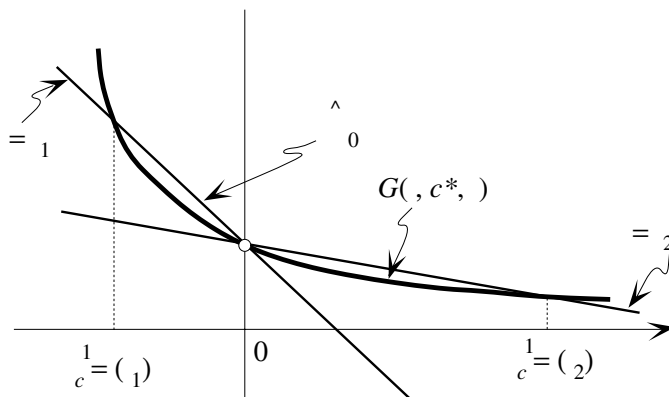


FIGURE 10. Graphs of $\hat{\zeta}_0^* - \tau\lambda$ and $G(\lambda, c^*, \tau)$.

eigenvalue $\lambda_c^{1,\varepsilon}(\tau)$ of $(LP)_{\varepsilon,\tau}$ at U^ε under the assumption (3.19) with $\lim_{\varepsilon \downarrow 0} \lambda_c^{1,\varepsilon}(\tau) = \lambda_c^1(\tau)$.

Remark 3.5. Suppose that U^ε has *more than one* transition layer like Figure 3 and there appear *more than two* critical eigenvalues in proportion to the number of layers. In fact, for the double layer case, there exist four critical eigenvalues including the zero translation free one, and two of them cross the imaginary axis like Figure 5, when τ decreases. Therefore, we have a layer oscillation of the double layer similar to Figure 3(b). We shall discuss this more precisely elsewhere.

4. Relation between layer oscillations and traveling waves.

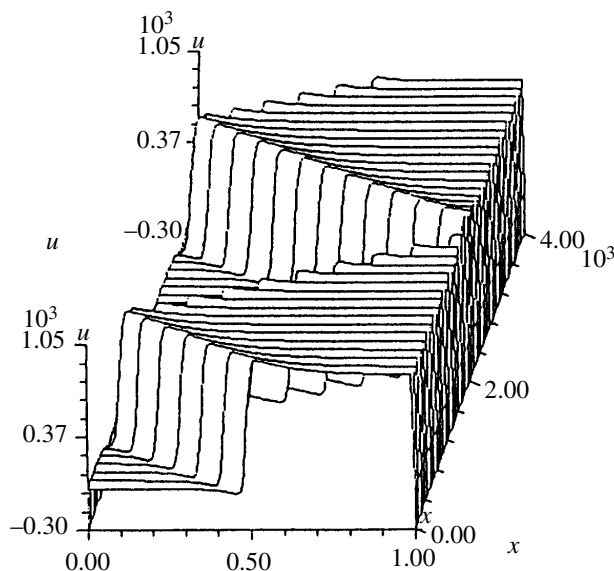
The difference of bifurcation phenomena between finite and infinite intervals is apparent from the results of previous sections. There appeared layer oscillations via Hopf bifurcation on a finite interval, while degenerate simple bifurcation to traveling waves (or its imperfection) occurred on an infinite line. The intuitive reason for this difference is rather clear. Namely, since there is no boundary for the case of the infinite line, the destabilized fronts (or backs) can proceed as far as they want instead of oscillating back and forth as in the finite

interval case. In fact, in view of Figure 11 which shows a large amplitude layer oscillation for small τ , we see that the shape of the solution almost looks like a traveling front when it proceeds from one end to the other. In other words, the symmetry of shift invariance on \mathcal{R} enables the destabilized fronts (or backs) to become traveling waves.

However, it is not straightforward to understand mathematically how the *Hopf bifurcation* becomes the degenerate *static bifurcation* of traveling type, when the length of the interval tends to infinity. The aim of this section is to give a rigorous description about the dependency of the behavior of critical eigenvalues on the length of the interval (Theorem 4.1). We shall see how two critical eigenvalues which cause layer oscillation are deformed continuously into a real simple eigenvalue plus zero translation free eigenvalue. It should be noted here that *not* all stationary solutions on a finite interval can be extended to those on \mathcal{R} satisfying (3.3) when the length goes to infinity. In fact, such cases occur only for a special class of nonlinearities, even if we restrict them to the bistable type (see the next subsection). However, we are able to obtain a deep insight through this narrow window about the change of the manner of the destabilization as the length tends to infinity. In this section we attach the super (or sub)script \hat{l} ($\equiv l^{-1}$) to the solutions and the interval such as $\mathcal{U}^{\varepsilon, \hat{l}}$ and $I_{\hat{l}}$ to put emphasis on the dependency of them on the length l of the interval.

4.1. *Convergence of the stationary solutions on finite interval to the standing front on \mathbf{R} .* For a fixed diffusion coefficient for v (recall that we already fixed D to be one), singularly perturbed stationary solutions of $(P)_{\varepsilon, \tau}$, in general, cease to exist when the length of the interval is sufficiently large ([7]). However, if the nonlinearities are of *bistable* type and are *odd symmetric* with respect to the middle equilibrium point R (Figure 7(b)), we can construct a one-parameter family of stationary solutions of $I_{\hat{l}}$ for fixed diffusion coefficients, which converge to the *standing front* on \mathbf{R} satisfying (3.3). Note that as far as the existence of stationary solutions of $(P)_{\varepsilon, \tau}$ is concerned, the parameter τ does not appear explicitly.

Lemma 4.1. (Existence of SP solutions converging to the standing front on \mathbf{R}). *Suppose that the nonlinearities f and g are of bistable type and odd symmetric with respect to the middle equilibrium point R*

FIGURE 11. Layer oscillation for sufficiently small τ .

(see Figure 7(b)). Then there exists a \hat{l} -parameter family of stationary solutions $\mathcal{U}_s^{\varepsilon, \hat{l}}(x) = (u_s^{\varepsilon, \hat{l}}(x), v_s^{\varepsilon, \hat{l}}(x))$ of $(P)_{\varepsilon, \tau}^{\hat{l}}$ on $I_{\hat{l}}$ which are odd symmetric at $x = 0$ and satisfy $\mathcal{U}_s^{\varepsilon, \hat{l}}(0) = R$. On the other hand, under the same assumption, $(P)_{\varepsilon, \tau}^0$ has a standing front $\mathcal{U}_s^{\varepsilon, 0} = (u_s^{\varepsilon, 0}(x), v_s^{\varepsilon, 0}(x))$ (i.e., traveling front solution of (3.2) with zero velocity) satisfying (3.3). Moreover, $\mathcal{U}_s^{\varepsilon, \hat{l}}$ converges to $\mathcal{U}_s^{\varepsilon, 0}$ in the following sense as $\hat{l} \rightarrow 0$:

$$(4.1) \quad \lim_{\hat{l} \downarrow 0} \sup_{x \in [-\hat{l}^{-1}, \hat{l}^{-1}]} \left| \frac{d^k}{dx^k} \mathcal{U}_s^{\varepsilon, \hat{l}} - \frac{d^k}{dx^k} \mathcal{U}_s^{\varepsilon, 0} \right| = 0$$

and

$$(4.2) \quad \left\{ \sup_{x \in [-\hat{l}^{-1}, 0]} \left| \frac{d^k}{dx^k} (U_s^{0, \hat{l}} - U_s^{0, 0}) \right| + \sup_{x \in [-\hat{l}^{-1}, 0]} \left| \frac{d^k}{dx^k} (V_s^{0, \hat{l}} - V_s^{0, 0}) \right| \right\} \leq C \exp(-\gamma/\hat{l})$$

for any nonnegative integer k , where $(U_s^{0, \hat{l}}, V_s^{0, \hat{l}})$ (respectively, $(U_s^{0, 0}, V_s^{0, 0})$) is the reduced (or outer) solution of $(P)_{\varepsilon, \tau}^{\hat{l}}$ (respectively, $(P)_{\varepsilon, \tau}^0$),

and C and γ are positive constants independent of small \hat{l} (see Theorem 2.1 and (3.10)). It is clear from the odd symmetry that the same estimate also holds on $[0, \hat{l}^{-1}]$.

Proof. In view of the construction of traveling fronts in [11], and using the odd symmetry, one can construct $\mathcal{U}_s^{\varepsilon, \hat{l}}$ and $\mathcal{U}_s^{\varepsilon, 0}$ without any difficulty. In fact, it suffices to construct them on the half of the interval with Dirichlet boundary condition $\mathcal{U}_s^{\varepsilon, \hat{l}}(0) = R$. We leave the details to the reader. As for the estimate (4.1) and (4.2), we only show (4.2) since (4.1) can be verified without any difficulty from (4.2) and its construction. Also note that it suffices to prove that the V -component is majorized by $\text{const} \cdot \exp(-\gamma/\hat{l})$ since the U -component $U_s^{0, \hat{l}}$ (respectively, $U_s^{0, 0}$) is defined by $h_-(V_s^{0, \hat{l}})$ (respectively, $h_-(V_s^{0, 0})$). First note that $(V, V_x) = (v_-, 0)$ is a saddle equilibrium point of the differential equation $V_{xx} + G_-(V) = 0$ and that the orbit $(V_s^{0, 0}, (V_s^{0, 0})_x)$ is one branch of the stable manifold converging to $(v_-, 0)$. Therefore, $V_s^{0, 0}$ (respectively, $(d^k/dx^k)V_s^{0, 0}$, $k \geq 1$) converges to v_- (respectively, 0) as $x \rightarrow -\infty$ with the order $O(\exp(\gamma x))$ for some positive γ . Recalling that the orbital structure near $(v_-, 0)$ is diffeomorphic to the linearized saddle critical point, and noting that $V_s^{0, \hat{l}}$ satisfies $(V_s^{0, \hat{l}})_x(-\hat{l}^{-1}) = 0$ and $|V_s^{0, \hat{l}}(-\hat{l}^{-1}) - V_s^{0, 0}(-\hat{l}^{-1})| = O(\exp(-\gamma\hat{l}^{-1}))$, we see that the estimate (4.2) follows easily after some computation. \square

Since the standing front $\mathcal{U}_s^{\varepsilon, 0}$ does not depend on τ , the corresponding $G(\lambda; 0, \tau)$ of the SLEP equation (3.24) also does not depend on τ . Therefore, we write the right-hand side of (3.24) as $G(\lambda; 0)$ when $\mathcal{U}^\varepsilon = \mathcal{U}_s^{\varepsilon, 0}$. Thus, when τ varies, the change of stability occurs if and only if the straight line $\hat{\zeta}_0^* - \tau\lambda$ is tangent to $G(\lambda; 0)$ at $\lambda = 0$. This unique value of τ is equal to τ_c in Theorem 3.3. We denote the two critical eigenvalues of the SLEP equation at $\mathcal{U}_s^{\varepsilon, 0}$ by $\lambda_c^{0, 0}(\tau) (\equiv 0)$ and $\lambda_c^{1, 0}(\tau)$.

4.2. *Transition from layer oscillations to traveling fronts.* We shall study the behavior of eigenvalues of the SLEP equation at $\mathcal{U}_s^{\varepsilon, \hat{l}}$ as $\hat{l} \downarrow 0$. Our goal is the following.

Theorem 4.1. (Transition from layer oscillations to traveling fronts). Let $U_s^{\varepsilon, \hat{l}}$ (respectively, $U_s^{\varepsilon, 0}$) be the odd symmetric solution on $I_{\hat{l}}$ (respectively, the standing front on \mathbf{R}) in Lemma 4.1. Let $\lambda_c^{0, \hat{l}}(\tau)$ and $\lambda_c^{1, \hat{l}}(\tau)$ be two critical eigenvalues of the SLEP equation (2.18) for $U_s^{\varepsilon, \hat{l}}$ as in Theorem 2.1, and let $\lambda_c^{0, 0}(\tau) (\equiv 0)$ and $\lambda_c^{1, 0}(\tau)$ be two real critical eigenvalues of (3.24) at $U_s^{\varepsilon, 0}$ (see Theorem 3.3). Then it holds that

$$\lim_{\hat{l} \downarrow 0} \lambda_c^{0, \hat{l}}(\tau) = \lambda_c^{0, 0}(\tau) (\equiv 0)$$

and

$$\lim_{\hat{l} \downarrow 0} \lambda_c^{1, \hat{l}}(\tau) = \lambda_c^{1, 0}(\tau)$$

uniformly on any compact set of τ in $(0, +\infty)$. See Figure 12. Moreover, the SLEP equation (2.18) has no spectrum in \mathbf{C}_{μ_1} except those described as above, where μ_1 is a positive constant independent of small \hat{l} .

Proof. The proof is divided into three parts: Firstly, we show the convergence of the SLEP equation as $\hat{l} \downarrow 0$ (Lemma 4.2). Secondly, we unfold the critical eigenvalues of the SLEP equation for the standing front to small positive \hat{l} (Lemma 4.3). Finally, we show that there are no other spectrum except $\{\lambda_c^{i, \hat{l}}\}_{i=0}^1$ ($\hat{l} \geq 0$), which are important to stability and bifurcation (Lemma 4.4). Using these lemmas, Theorem 4.1 follows directly. \square

For later convenience, we write again the SLEP equations for $U_s^{\varepsilon, \hat{l}}$ and $U_s^{\varepsilon, 0}$ in the following form ((2.18) and (3.24)):

$$(4.3) \quad \hat{\zeta}_0^{*, \hat{l}} - \tau \lambda = G(\lambda; \hat{l})$$

$$(4.4) \quad \hat{\zeta}_0^{*, 0} - \tau \lambda = G(\lambda; 0).$$

Recall that the right-hand sides of (4.3) and (4.4) do not depend on τ .

Lemma 4.2. (Convergence of the SLEP equation).

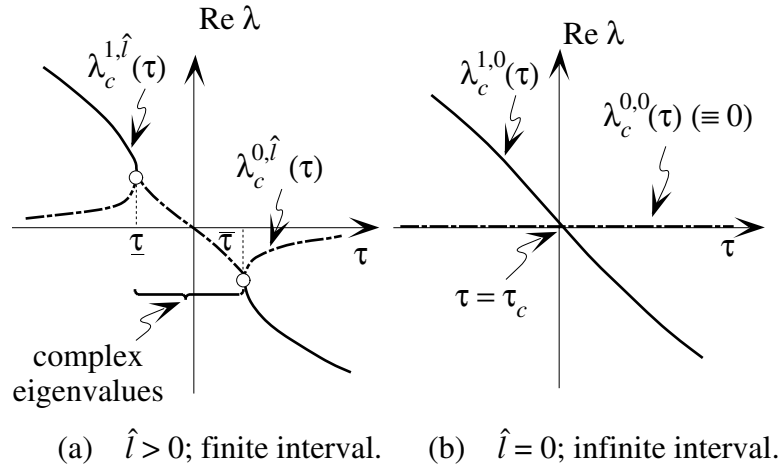


FIGURE 12. Behaviors of critical eigenvalues when \hat{l} tends to zero.

- (a) $\lim_{\hat{l} \downarrow 0} \hat{\zeta}_0^{*,\hat{l}} = \hat{\zeta}_0^{*,0} > 0$.
- (b) $\lim_{\hat{l} \downarrow 0} D^k G(\lambda; \hat{l}) = D^k G(\lambda; 0)$ uniformly on any compact subset in $\mathbf{C}_{\hat{\mu}}$ with respect to λ for any nonnegative k where $D \equiv \frac{d}{d\lambda}$.
- (c) $G(0; \hat{l}) \geq \hat{\zeta}_0^{*,\hat{l}}$ where the equality holds if and only if $\hat{l} = 0$.

Proof. (a) For the odd symmetric case, the velocity of the traveling front is equal to zero; therefore, the formula (3.25) becomes

$$\hat{\zeta}_0^{*,0} = \frac{dc_0(v^*)}{d\beta} \int_{-\infty}^0 g(U_s^{0,0}, V_s^{0,0}) dx,$$

where v^* is the equal area level, i.e., $J(v^*) = \int_{h_-(v^*)}^{h_+(v^*)} f(s, v^*) ds = 0$. Here we need the following sublemma.

Sublemma 4.1.

$$(4.5) \quad \frac{dc_0(\beta^*)}{d\beta} = \frac{\langle f_v(W, \beta^*), W_y^* \rangle}{\langle W_y, W_y^* \rangle}.$$

Proof. Recalling that $W(y; c_0(\beta), \beta)$ satisfies (see (3.12))

$$\frac{d^2}{dy^2}W - c_0(\beta)\frac{d}{dy}W + f(W, \beta) = 0.$$

Differentiating this with respect to β , we have

$$(4.6) \quad \frac{d^2}{dy^2}W_\beta - c_0(\beta)\frac{d}{dy}W_\beta + f_u(W, \beta)W_\beta - \frac{dc_0(\beta)}{d\beta}\frac{d}{dy}W + f_v(W, \beta) = 0.$$

Taking the inner product with W_y^* on both sides of (4.6) and using the fact that W_y^* satisfies

$$\frac{d^2}{dy^2}W_y^* + c_0(\beta)\frac{d}{dy}W_y^* + f_u(W, \beta)W_y^* = 0,$$

we obtain after integration by parts for $\beta = \beta^*$

$$-\frac{dc_0(\beta)}{d\beta}\langle W_y, W_y^* \rangle + \langle f_v(W, \beta^*), W_y^* \rangle = 0,$$

which shows (4.5). \square

For the odd symmetric case, the Sturm-Liouville operator L^ε becomes self-adjoint at the standing front, and, therefore, $W_y^* \equiv W_y$ holds. Therefore, the formula (4.5) can be rewritten in the following form

$$\frac{dc_0(v^*)}{d\beta} = \|W_y\|_{L^2}^{-2} \frac{dJ}{dv}(v^*).$$

Thus we have for the standing front case

$$\hat{\zeta}_0^{*,0} = \|W_y\|_{L^2}^{-2} \frac{dJ}{dv}(v^*) \int_{-\infty}^0 g(U_s^{0,0}, V_s^{0,0}) dx.$$

Recalling the formula (2.6) and noting that the switching point x_1^* becomes zero because of odd symmetry, the difference $\hat{\zeta}_0^{*,0} - \hat{\zeta}_0^{*,\hat{l}}$ is given by

$$\begin{aligned} \hat{\zeta}_0^{*,0} - \hat{\zeta}_0^{*,\hat{l}} &= \|W_y\|_{L^2}^{-2} \frac{dJ}{dv}(v^*) \\ &\quad \times \left\{ \int_{-\infty}^0 g(U_s^{0,0}, V_s^{0,0}) dx - \int_{-\hat{l}-1}^0 g(U_s^{0,\hat{l}}, V_s^{0,\hat{l}}) dx \right\}. \end{aligned}$$

Using Lemma 4.1 and that $g(U_s^{0,0}, V_s^{0,0})$ decays with the same exponential order as $x \rightarrow -\infty$, we see that

$$(4.7) \quad |\hat{\zeta}_0^{*,0} - \hat{\zeta}_0^{*,\hat{l}}| \leq C_1 \exp(-\gamma \hat{l}) \quad \text{as } \hat{l} \downarrow 0,$$

where C_1 and γ are positive constants independent of \hat{l} , which proves (a).

(b) Recalling the definitions of $G(\lambda; \hat{l})$ and $G(\lambda; 0)$ ((2.18) and (3.24)), it suffices to show the convergence of the Green kernel of the differential operator $T_\lambda^{\hat{l}}$ (see (2.12)) as $\hat{l} \downarrow 0$. One can easily prove this by using Lemma 4.1, so the details are left to the reader. Finally, (c) is the restatement of (2.2) and the second part of Lemma 3.4. \square

Remark 4.1. Lemma 4.2 says that the SLEP equation on a finite interval converges nicely to that on the whole line as $\hat{l} \downarrow 0$. Therefore, we can extend (4.3) to be valid up to $\hat{l} = 0$.

Our strategy for the study of the transition of solution structure as $\hat{l} \downarrow 0$ is to unfold the eigenvalues of the SLEP equation at the standing front to small but positive \hat{l} rather than tracing the asymptotic behaviors of them for $\mathcal{U}_s^{\varepsilon, \hat{l}}$.

Lemma 4.3. (Unfolding the zero eigenvalue of double multiplicity).

(a) *When $\tau = \tau_0$ is not equal to τ_c (see Theorem 3.3), there are two simple (transversal) zeros, $\lambda_c^{0,0}(\tau_0) (\equiv 0)$ and $\lambda_c^{1,0}(\tau_0)$ of (4.4) at $\mathcal{U}_s^{\varepsilon, 0}$. Each of them can be uniquely extended to positive \hat{l} in a continuous way as a real solution of (4.3) like $\lambda = \lambda_c^{i,\hat{l}}(\tau)$ ($i = 0, 1$) for $|\tau - \tau_0| < \delta_0$ and $0 \leq \hat{l} < l_0$ with $\lim_{\tau \rightarrow \tau_0, \hat{l} \rightarrow 0} \lambda_c^{i,\hat{l}}(\tau) = \lambda_c^{i,0}(\tau_0)$, where δ_0 and l_0 are appropriate positive constants.*

(b) *When $\tau = \tau_c$, (4.4) has a zero eigenvalue of double multiplicity. When \hat{l} becomes positive, this splits into two eigenvalues with the following principal parts:*

$$(4.8) \quad \lambda_{\pm} \simeq \frac{1}{2A} \left\{ -\hat{\tau} \pm \sqrt{(\hat{\tau})^2 - 4AC(\hat{l})} \right\} \quad \text{as } \hat{\tau} \text{ and } \hat{l} \text{ tend to zero,}$$

where $\hat{\tau} \equiv \tau - \tau_c$, $A \equiv \frac{1}{2} \frac{d^2}{d\lambda^2} G(0; 0)$ and $C(\hat{l}) \equiv G(0; \hat{l}) - \hat{\zeta}_0^{*,\hat{l}} \geq 0$ (Lemma 4.2(c)). Here λ_+ (respectively, λ_-) is equal to $\lambda_c^{1,\hat{l}}(\tau)$ (respectively,

$\lambda_c^{0,\hat{\lambda}}(\tau)$ in Theorem 2.3 (see also Remark 2.1). Moreover, any solution of (4.3) converging to zero as $\hat{l} \downarrow 0$ must be included in the above unfolding family of solutions.

Proof. In view of Remark 4.1, we see that the first part is easily obtained by applying the implicit function theorem to the SLEP equation at $\hat{l} = 0$. As for (b), we first expand $G(\lambda, \hat{l})$ near $(\lambda, \hat{l}) = (0, 0)$ as

$$(4.9) \quad G(\lambda; \hat{l}) = G(0, \hat{l}) - \tau_c \lambda + A\lambda^2 + (\text{h.o.t.}),$$

where $A = \frac{1}{2} \frac{d^2}{d\lambda^2} G(0; 0)$. Note that G does not depend on τ for the odd symmetric case since $\mathcal{U}_s^{\varepsilon, \hat{l}}$ remains as a steady state up to $\hat{l} = 0$. Therefore, (4.3) becomes

$$(4.10) \quad \hat{\zeta}_0^{*, \hat{l}} - (\hat{\tau} + \tau_c)\lambda = G(0; \hat{l}) - \tau_c \lambda + A\lambda^2 + (\text{h.o.t.}).$$

Applying the generalized Morse lemma to (4.10) at $(\lambda, \hat{\tau}, \hat{l}) = (0, 0, 0)$ (see Chap. 3, [16]), we have the asymptotic formula (4.8).

Finally, combining these two results, we can find an $\hat{l} = \hat{l}_1$ which is independent of $\tau \in \mathcal{K}$ such that $\{\lambda_c^{i,0}(\tau)\}_{i=0}^1$ can be extended uniquely to $\hat{l} = \hat{l}_1$ for $\tau \in \mathcal{K}$ where \mathcal{K} is an arbitrary compact set in $0 \leq \tau \leq \tau_1$ with τ_1 being an appropriate large positive constant. \square

The following lemma guarantees us that we can concentrate on the behaviors of $\{\lambda_c^{i,\hat{l}}(\tau)\}_{i=0}^1$ as $\hat{l} \downarrow 0$.

Lemma 4.4. *The SLEP equation (4.3) has no spectrum in \mathbf{C}_{μ_1} except $\{\lambda_c^{i,\hat{l}}(\tau)\}_{i=0}^1$ ($\hat{l} \geq 0$), where μ_1 is a positive constant independent of \hat{l} and τ .*

Proof. Let \hat{l} be an arbitrary fixed positive constant. It is clear that there are no other real solutions of (4.3) besides those obtained in Lemma 4.3 since the real solutions are given by the intersection points of two curves of (4.3). For complex eigenvalues, we first show that, for any real $\nu \geq 0$, there exists at most one λ satisfying (4.3) with $\text{Re } \lambda = \nu$ for an appropriate τ . Note that it suffices for us to consider only complex eigenvalues with positive imaginary parts.

Recalling Remark 2.1, we see that the SLEP equation (4.3) is equivalent to

$$(4.11)_a \quad \lambda_{\mathbf{R}} = \hat{\zeta}_0^{*,\hat{l}}/\tau - A/B$$

and

$$(4.11)_b \quad B = \tau.$$

Let $B_\nu = B(\nu, 0)$. In view of Sublemma 2.1(a), we see that there do not exist complex solutions of (4.11)_b for $\tau \geq B_\nu$. On the other hand, it follows from (a) and (b) of Sublemma 2.1 that there exists a unique solution $\lambda_I = \lambda_I(\tau; \nu)$ satisfying (4.11)_b with $\lambda_{\mathbf{R}} = \nu$ for any $\tau < B_\nu$. Note that $\lambda_I(\tau; \nu)$ is a strictly decreasing function of τ ($< B_\nu$) with $\lambda_I(B_\nu; \nu) = 0$ and $\lim_{\tau \downarrow 0} \lambda_I(\tau; \nu) = +\infty$. Substituting $\lambda_I(\tau; \nu)$ into (4.11)_a, we obtain the following scalar equation with respect to τ :

$$(4.12) \quad \hat{\zeta}_0^{*,\hat{l}} - \tau\nu = A(\nu, (\lambda_I(\tau; \nu))^2).$$

Using again Sublemma 2.1, we see that the right-hand side of (4.12) is strictly increasing with respect to τ for $0 < \tau < B_\nu$ while the left-hand side of (4.12) is a straight line with nonpositive slope with respect to τ for $\nu \geq 0$. Therefore, the solution of (4.12) (if it exists) is uniquely determined.

Remark 4.2. Suppose that the SLEP equation (4.3) has a real solution $\lambda = \nu$ for some τ , then it has no complex solutions λ with $\operatorname{Re} \lambda = \nu$. This can be verified by applying the monotonicity property of A to (4.12) (see Sublemma 2.1).

Using the above results, we can conclude by contradiction that there exists a positive constant $\mu_1(\hat{l})$ such that the SLEP equation (4.3) has no spectrum in $\mathbf{C}_{\mu_1(\hat{l})}$ except those in Lemma 4.3. However, $\mu_1(\hat{l})$ may depend on \hat{l} and there may exist a sequence of complex eigenvalues $\lambda(\hat{l})$ with $\operatorname{Re} \lambda(\hat{l}) < 0$ other than those in Lemma 4.3 which approach the imaginary axis as $\hat{l} \downarrow 0$. We can avoid this possibility by contradiction. First note that such a sequence remains bounded as $\hat{l} \downarrow 0$, namely $|\operatorname{Im} \lambda(\hat{l})| < M$ with M being independent of \hat{l} . This is

easily seen from (4.11), Sublemma 2.1, and Lemma 4.2(a). Therefore, we can choose a convergent subsequence $\{\lambda(\hat{l}_n)\}_{n \geq 1}$ ($\hat{l}_n \downarrow 0$ as $n \uparrow \infty$) with $\lim_{n \uparrow \infty} \operatorname{Re} \lambda(\hat{l}_n) = 0$. Then its limit $\lambda^* \equiv \lim_{\hat{l}_n \downarrow 0} \lambda(\hat{l}_n)$ on the imaginary axis becomes one of the solutions of the limiting SLEP equation (4.4) for the standing front. However, because of the uniqueness property of the critical eigenvalues on the imaginary axis λ^* must be equal to zero. However, this contradicts the uniqueness of the unfolding of zero eigenvalue of (4.4) to $\hat{l} > 0$ (see Lemma 4.3). This completes the proof of Lemma 4.4. \square

Acknowledgments. Several results in 2 and 3 as well as numerical pictures were obtained jointly with Professors M. Mimura, H. Ikeda, and H. Fujii as in the detailed papers [11, 20, and 21]. The author would like to thank them for their cooperation and generosity.

REFERENCES

1. G. Caginalp, *An analysis of a phase field model of a free boundary*, Arch. Rational Mech. Anal. **92** (1986), 205–245.
2. G.A. Carpenter, *A geometric approach to singular perturbation problem with application to nerve impulse equations*, J. Differential Equations **23** (1977), 335–367.
3. E.D. Conway, *Diffusion and predator-prey interaction: pattern in closed system*, Research Notes in Math. **101**, Pitman, (1984), 85–133.
4. G.B. Ermentrout, S.P. Hastings, and W.C. Troy, *Large amplitude stationary waves in an excitable lateral-inhibition medium*, SIAM J. Appl. Math. **44** (1984), 1133–1149.
5. P.C. Fife, *Propagator-controller systems and chemical patterns*, Non-equilibrium dynamics in chemical system (eds. C. Vical and A. Pacault), Springer Verlag, 1984, 76–88.
6. ——— and J.B. McLeod, *The approach of solutions of nonlinear diffusion equation to traveling wave solutions*, Arch. Rational Mech. Anal. **65** (1977), 335–361.
7. H. Fujii, M. Mimura and Y. Nishiura, *A picture of the global bifurcation diagram in ecological interacting and diffusing systems*, Phys. D **5** (1982), 1–42.
8. S. Hastings, *Some mathematical problems arising in neurobiology*, Mathematics of Biology, C.I.M.E. **1** (1981), 179–264.
9. D. Henry, *Geometric theory of semilinear parabolic equations*, Lecture Notes in Math. **840**, Springer Verlag, 1981.
10. Y. Hosono and M. Mimura, *Singular perturbation approach to traveling waves in competing and diffusing species models*, J. Math. Kyoto Univ. **22** (1982), 435–461.

11. H. Ikeda, M. Mimura, and Y. Nishiura, *Global bifurcation phenomena of traveling wave solutions for some bistable reaction-diffusion systems*, Nonlinear Anal. TMA **13** (1989), 507–526.
12. C.R.K. Jones, *Stability of the travelling wave solutions of the FitzHugh-Nagumo system*, Trans. Amer. Math. Soc. **286**, (1984), 431–469.
13. H. Meinhardt, *Models of Biological Pattern Formation*, Academic Press, 1982.
14. M. Mimura, Y. Kan-on and Y. Nishiura, *Oscillations in segregation of competing populations*, Proceedings of the Research Conference on Mathematical Biology, Trieste (eds. G. Hallam, L.J. Gross and S.A. Levin), Worldscientific (1988), 717–733.
15. ———, M. Tabata and Y. Hosono, *Multiple solutions of two-point boundary value problems of Neumann type with a small parameter*, SIAM J. Math. Anal. **11** (1981), 613–631.
16. L. Nirenberg, *Topics in nonlinear functional analysis*, Courant Inst. Math. Sci. Notes, 1972/73.
17. Y. Nishiura, *Stability analysis of traveling front solutions of reaction-diffusion systems—An application of the SLEP method*, manuscript.
18. ——— and H. Fujii, *Stability of singularly perturbed solutions to systems of reaction-diffusion equations*, SIAM J. Math. Anal. **18** (1987), 1726–1770.
19. ——— and ———, *SLEP method to the stability of singularly perturbed solutions with multiple internal transition layers in reaction-diffusion systems*. Proc. of NATO Advanced Research Workshop “Dynamics of Infinite Dimensional Systems,” Lisbon (eds. J.K. Hale and S.N. Chow), NATO ASI Series F-37, 1986, 211–230.
20. ——— and M. Mimura, *Layer oscillations in reaction-diffusion systems*, SIAM J. Appl. Math. **49** (1989), 481–514.
21. ———, ———, H. Ikeda and H. Fujii, *Singular limit analysis of stability of travelling wave solutions in bistable reaction-diffusion systems*, SIAM J. Math. Anal. **21** (1990), 85–122.
22. J. Rinzel and D. Terman, *Propagating phenomena in a bistable reaction-diffusion system*, SIAM J. Appl. Math. **42** (1982), 1111–1137.
23. J.J. Tyson and P.C. Fife, *Target patterns in a realistic model of the Belousov-Zhabotinskii reaction*, J. Chem. Phys. **73**, (5), (1980), 2224–2237.
24. E. Yanagida, *Stability of fast travelling pulse solutions of the FitzHugh-Nagumo equations*, J. Math. Biol. **22** (1985), 81–104.

FACULTY OF INTEGRATED ARTS AND SCIENCES, HIROSHIMA UNIVERSITY, HIROSHIMA 730, JAPAN